1 **Size-Dependent Protein-Nanoparticle Interactions in Citrate-Stabilized**

2 **Gold Nanoparticles: The Emergence of the Protein Corona**

3 Jordi Piella[a,b], Neus G. Bastús[a] and Víctor Puntes[a,c,d]*

4 [a] Institut Català de Nanociència i Nanotecnologia (ICN2), CSIC and The Barcelona Institute of Science and

5 Technology (BIST), Campus UAB, 08193 Bellaterra, Barcelona, Spain.

6 [b] Universitat Autònoma de Barcelona (UAB), Campus UAB, 08193 Bellaterra, Barcelona, Spain

7 [c] Institució Catalana de Recerca i Estudis Avançats (ICREA), P. Lluís Companys 23, 08010 Barcelona, Spain
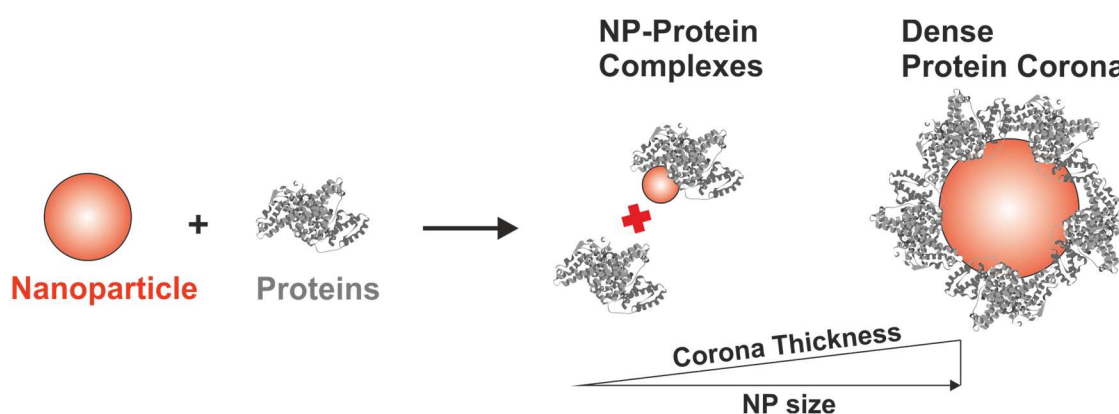
8 [d] Vall d'Hebron Institut de Recerca (VHIR), 08035 Barcelona, Spain

9 * To whom correspondence should be addressed: E-mail: victor.puntes@icn2.cat

10 **Abstract**

11 Surface modifications of highly monodisperse citrate-stabilized gold nanoparticles (AuNPs) with
12 sizes ranging from 3.5 to 150 nm after their exposure to cell culture media supplemented with fetal
13 bovine serum were studied and characterized by the combined use of UV-vis spectroscopy, dynamic
14 light scattering, and zeta potential measurements. In all the tested AuNPs, a dynamic process of
15 protein adsorption was observed, evolving toward the formation of an irreversible hard protein
16 coating known as the Protein Corona. Interestingly, the thickness and density of this protein coating
17 were strongly dependent on the particle size, making it possible to identify different transition regimes
18 as the size of the particles increased: (i) NP-protein complexes (or incomplete corona), (ii) the
19 formation of a near-single dense protein corona layer, and (iii) the formation of a multilayer corona.
20 In addition, the different temporal patterns in the evolution of the protein coating come about more
21 quickly for small particles than for the larger ones, further revealing the significant role that size plays
22 in the kinetics of this process. Since the biological identity of the NPs is ultimately determined by the
23 protein corona and different NP-biological interactions take place at different time scales, these results
24 are relevant to biological and toxicological studies.

25 **TOC**

26

Introduction

Noble metal nanoparticles (NPs) are among the most widely used nanomaterials in biomedicine because of their outstanding optical, electromagnetic, and photothermal properties. These unique properties, together with the high reactivity of the NPs and their affinity for binding many different (bio)molecules, make them attractive candidates in a wide variety of uses and applications including delivery, diagnostics, and therapy.[1][2] However, despite the rapid development of strategies for particle design and functionalization, relatively little is known about their *in vitro* and *in vivo* behavior in complex biological systems.[3]

The ability to integrate NPs in biological systems ultimately relies on the fundamental understanding of the interaction of these inorganic NPs with biological fluids.[4-6] A large number of biological fluids (plasma serum or otherwise) are complex aqueous media composed of electrolytes, proteins, lipids, and metabolites, able to adsorb (by electrostatic, hydrophobic, van der Waals, and dispersive forces) onto the surfaces of the NPs forming a protein dense coating known as Protein Corona (PC),[7-11] a phenomena extensively studied previously in implants.[12] The PC shields the original surface properties of the NPs acting as a "complex" surfactant, and alters their size and composition providing the NPs with a new biological identity.[10, 13, 14] This corona is what is ultimately "seen" by cells, and critically determines the physiological response and interaction of the NPs with living systems, including cellular uptake, circulation lifetime, signaling, biodistribution, therapeutic effects, and toxicity.[15-21]

The composition, structure and kinetics of the PC formation depends on (i) the specific characteristics of the biological environments in which NPs are dispersed, especially protein composition[22] and concentration;[16, 23] (ii) the physicochemical features of the dispersed material, such as NP chemical composition[24], morphology,[7, 25, 26] surface charge (functional groups),[16, 27] and hydrophobicity,[7, 28] and (iii) the exposure time, which directly correlates with the relative abundance of proteins and the different protein-NP binding constants (Vroman's effect).[24, 27, 29] Among these parameters, the morphology of the NPs relating to size and shape has been suggested to play an important role. Due to surface curvature effects,[30] molecules tend to adopt different conformations on top of NPs as compared to flat surfaces indicating different protein-binding affinities, giving rise variation of the structure of PC according to the size of the NPs.[31] Pioneering studies were performed by Cerdervall et al.[7, 32] who investigated the role of surface curvature in copolymer NPs of 70 and 200 nm after their dispersion in plasma, and further studies were later extended to other sizes and compositions including AuNPs,[22, 33-35] AgNPs,[20] polystyrene NPs,[36-38] SiO$_2$,[14, 15, 25, 36] metal oxide NPs,[24, 39, 40] and polymer-coated FePt and CdSe/ZnS.[41] Although all of the authors reported consistent results, it was often difficult to separate the effect of NP size from other physicochemical aspects, such as particle composition and surface chemistry. Some of them found that particle size and surface curvature influences the amount of bound protein and (to a lesser extent) the identity of these proteins.[15, 25, 32] In

63   contrast, other studies reported significant qualitative size-dependent changes in protein adsorption.[40]

64   So far, the underlying mechanism explaining size-dependent protein-particle specific interaction is not

65   yet resolved. Moreover, in all these studies the diameter of the tested NPs was above that of most

66   abundant serum proteins (6-12 nm). As a result, changes in the PC of NPs of a similar or even smaller

67   size than proteins were not addressed. In this regard, only a few studies have provided data on this

68   size regime, including AuNPs (2 nm,15 nm),[16, 22] CdSe/ZnS (9-11nm),[42] and FePt (10 nm).[41]

69   Little is known about the PC formation of NPs when they are smaller than most of the proteins

70   themselves, with subsequent lack of knowledge of their biological consequences. Smaller NPs present

71   some features that make them very attractive for biomedical applications: they are less prone to

72   opsonization and have substantially longer lifetimes in the bloodstream, in such a way that a particle

73   as small as 10 nm would not significantly activate the immune system.[43, 44] They also have faster

74   biodegradation (e.g., dissolution) together with excretion profiles which may avoid unwanted

75   bioaccumulation.[45] Moreover, the small size of the NP may affect the PC formation process. Thus,

76   when NPs have sizes similar to (or even smaller than) those of proteins it may be difficult to form a

77   compact corona since the number of proteins at the surface of the particle is too small for a crowding

78   cooperative effect to be achieved.[24, 46] Conversely, as the size of the particles becomes larger, it may

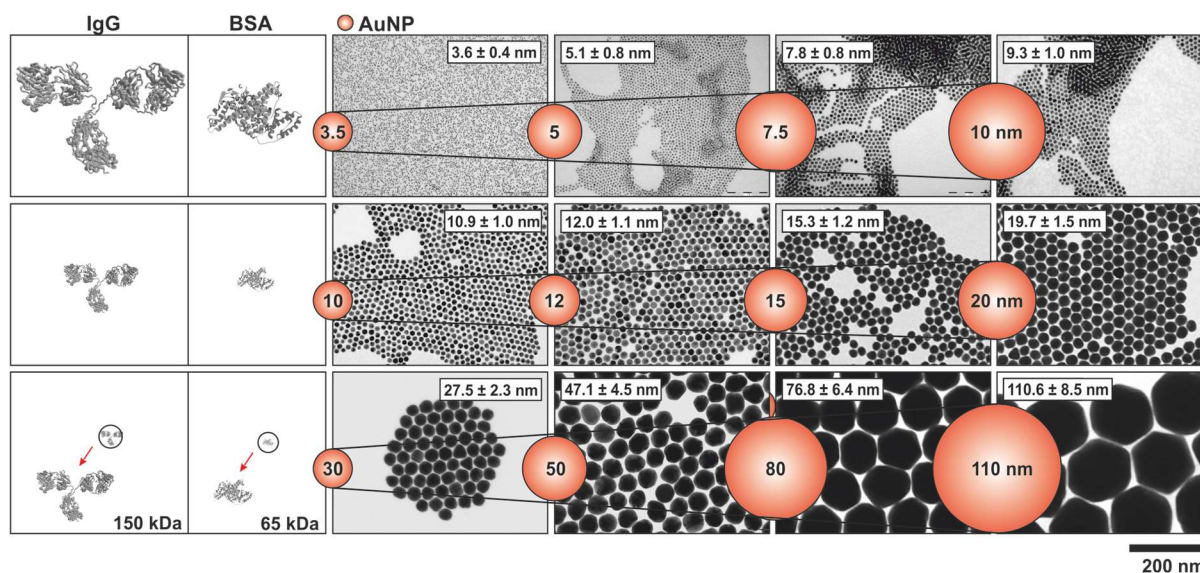79   be possible for a proper full density protein corona to develop.

80   Taking advantage of the recent improvements in the synthesis of sub-10 nm AuNPs,[47, 48] we have

81   studied the formation of PC on highly monodisperse citrate-stabilized AuNPs of different sizes (from

82   3.5 to 150 nm) after their exposure to cell culture media (CCM) supplemented with fetal bovine serum

83   (FBS). By the combined use of UV-vis spectroscopy, dynamic light scattering, and zeta potential, a

84   dynamic process of protein adsorption has been identified and characterized for all the tested particles,

85   leading to the formation of an irreversible coating that mediates the colloidal stability of the AuNPs in

86   the physiological medium. Interestingly, the thickness (and compactness) of this protein coating was

87   strongly determined by the size of the NPs being possible to identify a transition regime from AuNP-

88   complexes (or spare corona) in which the thickness of the corona was smaller than that expected for a

89   single protein layer (AuNPs ≤ 12 nm), to the formation of a full corona composed by a dense protein

90   monolayer for AuNPs sizes from 12 to 80 nm. Finally, for very large particles (> 80 nm), an

91   additional regime could be identified in which a multilayered corona composed of 2-3 protein layers,

92   similar to that reported in flat surfaces, seemed to be favored.[49]

93   **Results and Discussion**

94   The protein adsorption process was studied by incubating citrate-stabilized AuNPs for 48 h at 37^0C in

95   complete cell culture media (cCCM); composed of Dulbecco's Modified Eagle Medium (DMEM)

96   supplemented with 10% of fetal bovine serum (FBS). Highly monodisperse citrate-stabilized AuNPs

97   with sizes ranging from 3.5 to 150 nm were synthesized following recently reported kinetically-

98   controlled seeded-growth approaches.[47, 48] Citrate is a biocompatible reducer commonly used in the
99   synthesis of AuNPs which provides a negative electrostatic stabilization once adsorbed on the NP
100 surface. Besides, different from other surfactants that hinder the formation of the protein corona (PC),
101 i.e., polyethylene glycol (PEG),[26, 50, 51] the citrate layer is easily replaced, allowing the spontaneous
102 adsorption of proteins under normal conditions of *in vitro* and *in vivo* exposure.[50, 52] Moreover, FBS
103 is a biological fluid that contains more than 3700 different proteins, with 12 orders of magnitude
104 difference in their relative concentrations.[7] Among all proteins in serum, albumin represents the most
105 abundant fraction and accounts for ~60% in mass of the total proteins in solution (1 mM), with
106 globulins the second most abundant (~40%) and all the rest representing less than 1%.[52] With this in
107 mind, in Figure 1 the relative size of the particles used in this study is compared to proteins, using
108 bovine serum albumin (BSA) and Immunoglobulin G (IgG) as model proteins.

109 For the study of the PC formation, it is important to previously select the proper exposure condition of
110 the AuNPs in cCCM. cCCM is a high ionic strength medium in which the stability of citrate-coated
111 AuNPs is strongly compromised due to the screening of the electrostatic repulsion between particles
112 by the high concentration of charges in solution. This process is evidenced when performing exposure
113 experiments in DMEM media (**Fig. 2A**), where the immediate aggregation of 10 nm AuNPs is clearly
114 observed by UV-vis spectroscopy.[53] Thus, in the absence of serum proteins, the localized surface
115 plasmon resonance (LSPR) band of the particles rapidly vanishes, red-shifts and broadens, and a new
116 band between 600 and 800 nm emerges, which can be univocally ascribed to the coupling of the
117 plasmon modes of individual NPs when they come into contact.[52, 54]
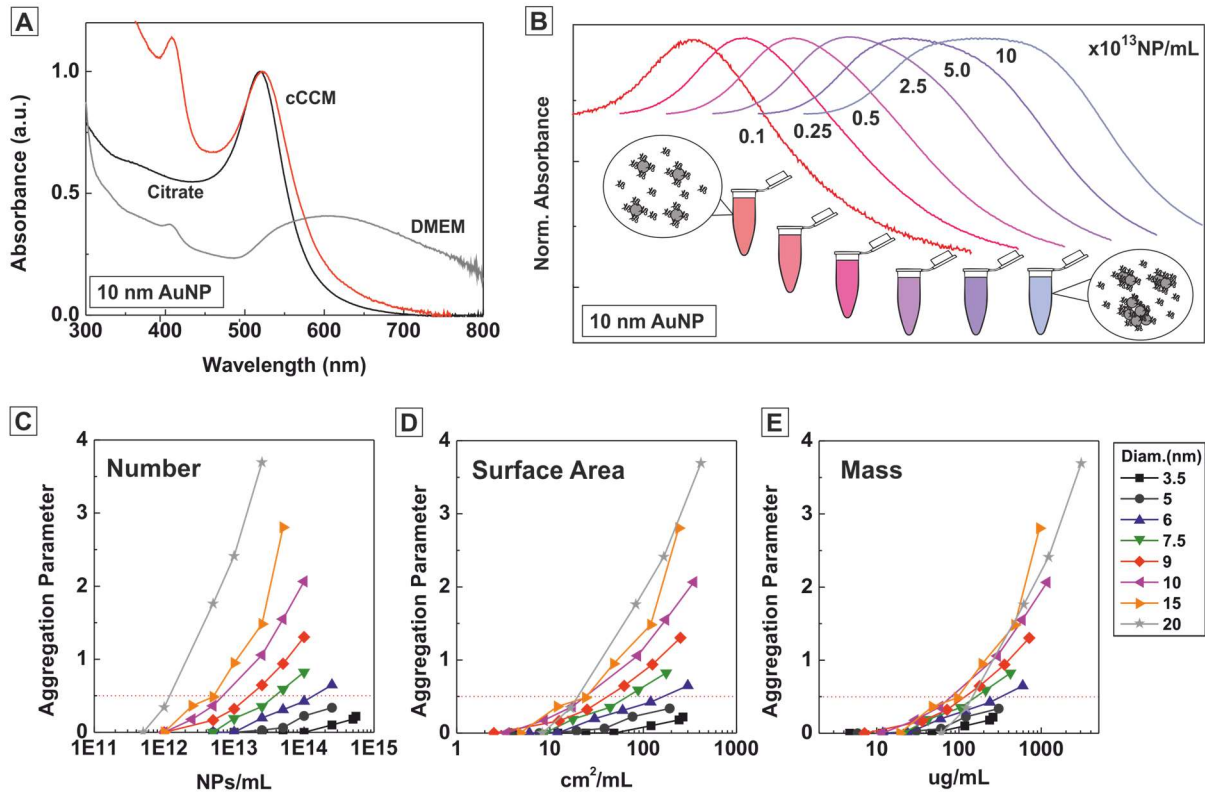

118
119 **Figure 1. Representative TEM images of citrate-stabilized AuNPs of selected sizes used in this study.** The
120 relative difference in size between AuNPs and proteins has been compared by choosing BSA (65 kDa) and IgG
121 (150 kDa), the two most abundant protein in serum, as model proteins. The inset spheres represent the size of
122 the AuNPs scaled to the model proteins schematically drawn in the column on the left. The smallest AuNPs (3.6
123 nm) cannot accommodate more than 1-2 proteins while AuNPs larger than 30 nm can accommodate hundreds of
124 them on their surfaces.

125   In the presence of proteins (fixed at the level of standard *in vitro* studies), particle concentration is the

126   main driver for aggregation. Stability conditions of 10 nm AuNPs in cCCM were initially studied by

127   exposing the same volume (1 mL) of particles of adjusted concentrations (from 10^{12} NP/mL to 10^{15}

128   NP/mL) to an equal volume of cCCM (9 mL), thus keeping the concentration of proteins constant

129   (**Fig. 2B**). The extent of aggregation was systematically quantified from UV-vis spectra, by

130   calculating the aggregation parameter (AP) according to Lévy *et al.*[54] after 1 h of exposure. AP values

131   higher than 0.5 indicated significant aggregation. It is important to note that the LSPR peak and the

132   calculation of this parameter were not affected by the presence of free protein in solution, since

133   proteins absorb at wavelengths far lower than the characteristic AuNPs band. For the selected NP-

134   protein exposure conditions, AuNPs were stable in cCCM at a low concentration of 2.5 10^{12} NPs/mL

135   while they formed aggregates when the concentration was increased above 2.5 10^{13} NPs/mL. Since the

136   concentration of proteins in the media does not represent a limiting factor (in all conditions the

137   amount of proteins in solution is largely above that needed to fully cover all available NP surface), the

138   aggregation is likely due to kinetic factors when mixing both solutions. That is, NPs destabilize and

139   aggregate before proteins succeed in protecting their surfaces.

140   When the NP and the protein solutions are mixed, two different kinetic processes are competing at the

141   same time: (i) the destabilization (and further aggregation) of the NPs promoted by the high ionic

142   strength of the media in which they are dispersed and (ii) the stabilization of the NP surface against

143   aggregation via protein adsorption. Thus, if the formation of a protective protein layer is faster than

144   the characteristic time of destabilization (that is the time needed by two individual "bare" particles to

145   bind to each other), then the resultant colloidal solution will remain stable. Conversely, the sample

146   will destabilize and (partially or totally) agglomerate, forming aggregates immediately coated by

147   proteins that will progressively sediment.[55] Based on these results, it becomes clear that these two

148   processes take place in the same time scale. For completeness, stability conditions were additionally

149   evaluated for particles of different sizes (3.5 to 20 nm) and the results were normalized to: (1) the total

150   number of NPs in solution (**Fig. 2C**), (2) the total surface area exposed by the NPs (**Fig. 2D**) and (3)

151   the total gold mass in each sample (**Fig. 2E**), with it being possible to observe that curves hardly

152   converge in any case. Only when the results were normalized to the total gold mass in each sample

153   did they become comparable, which suggest that, in excess of free proteins, the aggregation of the

154   particles is not exclusively determined by the probability of collisions of two individual particles but

155   may be affected by additional parameters. Interestingly, small particles appear to be slightly more

156   stable than large ones and thus are able to reach higher concentrations. This could be related to faster

157   protein coating or a faster dispersion of the NP due to increased Brownian motion as size decreases.

158   Consequently, stability conditions depend on both the characteristics of the AuNPs and the ratio

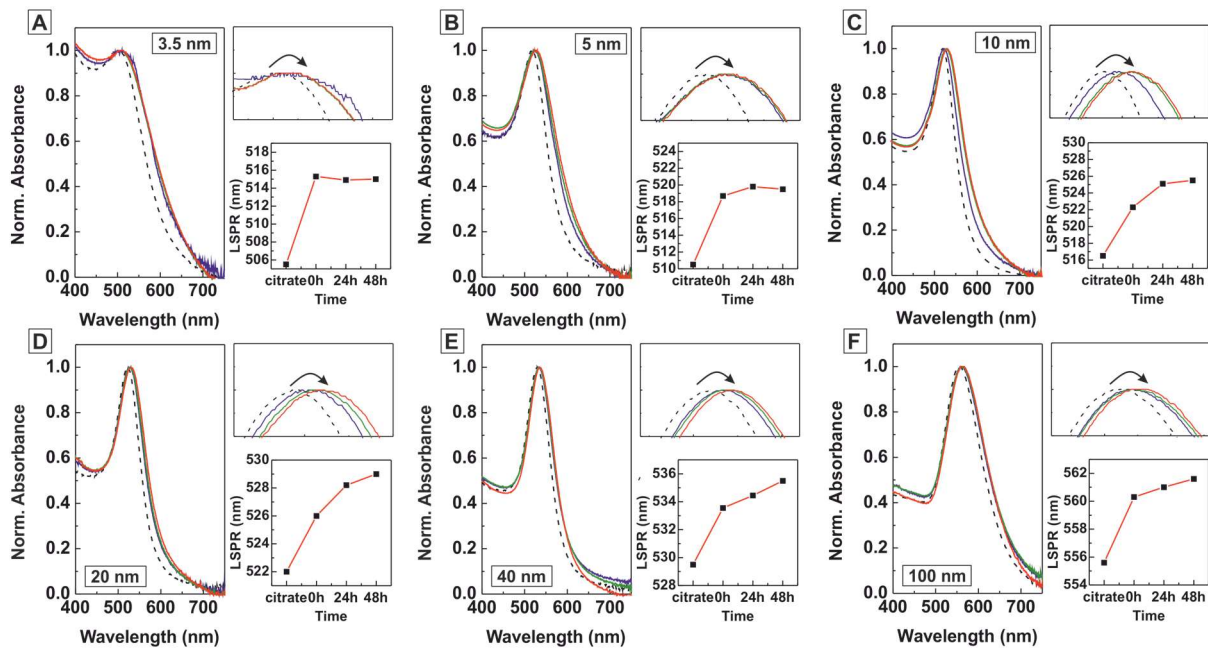159   between the NPs and protein concentration in the media.

160

Figure 2. Optimization of exposure conditions. (A) UV-vis spectra of AuNPs in different media. AuNPs aggregate in DMEM, even at low particle concentration, while they remain stable in cCCM. (B) Normalized UV−vis spectra of AuNPs in cCCM at different concentrations. The changes in the LSPR band indicate that AuNPs aggregate in cCCM when they were exposed to the medium at high concentration while their stability was not compromised at low concentration. (C-E) Experimentally measured aggregation parameter of AuNPs of different sizes after their exposure to cCCM at increasing NP concentrations. Results are normalized by particle number (NPs/mL) (C), total particle surface area (cm^2/mL) (D) and total mass of Au atoms (μg/mL) (E). In all cases 1 mL of a solution of AuNPs 10x concentrated with respect to the desired concentration was added to 9 mL of the medium and rapidly mixed for a couple of minutes before being left undisturbed for 1 h under mild stirring.

Considering these results, we adjusted the concentration of AuNPs, from ~10^{13} NPs/mL for the smallest particles (3.5 nm) to ~10^9 NP/mL for the largest ones (150 nm), to be low enough to promote the formation of a protein layer before the characteristic time of destabilization. It is worth mentioning that these studies show how the exposure of NP to physiological media is concentration dependent and how dispersion of highly concentrated NP samples in these media (as i.v. injection or high NP dose toxicology studies) may be challenging.

Protein adsorption profile is a kinetic process in which a soft protein corona composed of loosely bound proteins in equilibrium with the free proteins in solution initially forms and evolves slowly toward an irreversible hard protein corona consisting of tightly bound proteins that do not readily desorb.[24] In this process, the proteins adsorb/desorb and rearrange at the surface of the particle, leading to the hardening of the corona, a process that determines the final identity of the particle. In this stable (hard) conformation of the protein corona, crowding/cooperative effects between attached proteins are a key factor: once the protein layer is formed, the incorporation of a new protein implies

Figure 3. UV-vis characterization of purified AuNPs of selected sizes after their exposure to cCCM for different times: (A) 3.5 nm, (B) 5 nm, (C) 10 nm, (D) 20 nm, (E) 40 nm, (F) 100 nm. UV-Vis spectra before (dotted-line) and after their exposure at different times (blue t<30 min, green t=24 h, red t=48 h).

the rearrangement of many, which is translated into a highly stable PC. This process takes about 48 h in the case of AuNPs that end up having a permanent PC that does not detach from the surface when NPs are redispersed in protein-free media.[27] To obtain a PC hardening profile, the NP has to be purified from the exposure media to remove the unbound and loosely bound proteins, which is indeed a critical step. Purification of the AuNPs was performed by centrifugation followed by subsequent dispersion in protein-free aqueous solution after a proper optimization of the process. Additionally, the number of purification steps was determined to be at least 2. Otherwise the presence of unbounded free proteins was directly translated into bimodal size distributions in dynamic light scattering (DLS) measurements, in particular for the small nanoparticles (more details can be found in the SI).

The size-dependent evolution of the hardening of the protein corona was analyzed by UV-vis spectroscopy, DLS, and zeta potential measurements of purified samples. This combination of characterization techniques provides a remarkably robust analysis of the interaction between the proteins and the NPs in the colloidal state,[27] bypassing complex postprocessing steps and/or avoiding chemical labeling strategies, such as luminescent or radioactive labelling, usually needed for protein detection. As observed in **Table 1**, important changes in the physicochemical properties of the purified AuNPs after exposure to cCCM are identified. The LSPR band of the AuNPs systematically red-shifts which can be ascribed to the change of the refractive index at the vicinity of the particles[56], and it is consistent with the spontaneous binding of media proteins.[27, 51] The shift is clearly observed within minutes and it takes 24-48 h to reach a stationary value, indicating a dynamic process of hardening of the protein corona, reaching a constant value faster for small particles than for the large

209 ones **(Fig. 3)**. The extent of the red-shift also depends on particle size being $\Delta\lambda \approx 9$ nm for the

210 smallest AuNPs (3.5 nm) and $\Delta\lambda \approx 6$ nm for the largest ones (150 nm). However, this cannot be

211 directly correlated with the thickness and density of the protein layer since particles of different sizes

212 present different sensitivity toward similar modifications of the surrounding environment (thickness,

213 refractive index and chemical anchoring).[56] The absence of absorbance peaks at longer wavelengths is

214 further evidence that under optimized conditions the AuNPs remain stable and well-dispersed in
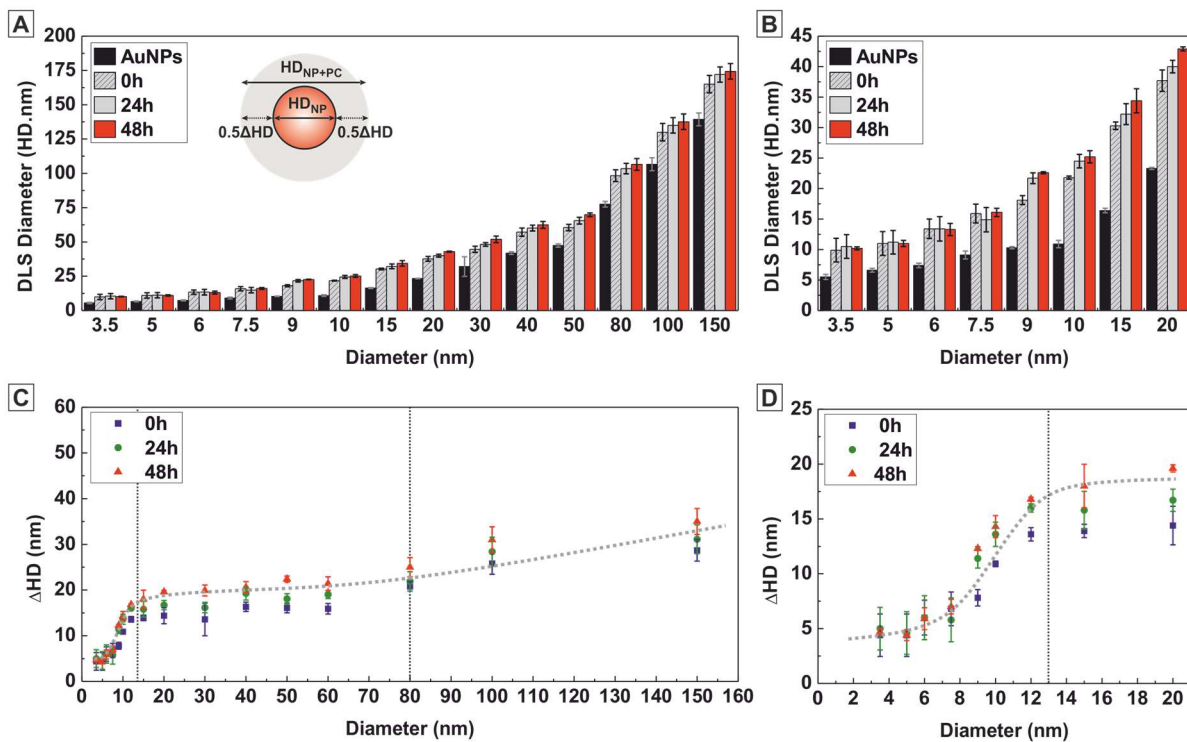
215 cCCM for all the sizes under study.[54]

216 **Table 1. Physicochemical Characterization of AuNPs before and after Exposure to cCCM for 48 h and**
217 **Further Purified.**

target Size (nm)	citrate				cCCM		
	diameter TEM (nm)	diameter DLS (nm)	ζ-Potential (mV)	LSPR maximum (nm)	diameter DLS (nm)	ζ-Potential (mV)	LSPR maximum (nm)
3.5	3.6 ± 0.4	5.5 ± 1.2	-36.8 ± 8.7	505.5	10.2 ± 3.9	-32.8 ± 5.1	515.0
5	5.1 ± 0.8	6.6 ± 1.4	-37.2 ± 14.3	510.5	11.0 ± 3.6	-31.0 ± 7.8	519.5
6	6.2 ± 0.6	7.4 ± 1.6	-39.6 ± 11.1	513.0	13.3 ± 3.2	-26.1 ± 4.3	522.5
7.5	7.8 ± 0.8	9.1 ± 1.9	-42.6 ± 8.6	515.0	16.1 ± 4.3	-24.5 ± 6.2	523.5
9	9.3 ± 1.0	10.3 ± 2.2	-43.6 ± 19.8	516.0	22.6 ± 4.1	-22.5 ± 5.1	524.0
10	10.9 ± 1.0	10.9 ± 3.4	-45.8 ± 14.6	516.5	25.2 ± 5.3	-16.7 ± 5.3	525.5
12	12.0 ± 1.1	12.9 ± 2.7	-42.9 ± 16.4	516.5	29.7 ± 6.9	-16.5 ± 4.8	524.0
15	15.3 ± 1.2	16.4 ± 3.5	-42.9 ± 17.3	518.5	34.4 ± 8.3	-17.1 ± 4.6	527.0
20	19.7 ± 1.5	23.3 ± 4.8	-46.9 ± 15.6	522.0	42.9 ± 9.3	-18.9 ± 6.5	529.0
30	27.5 ± 2.3	32.0 ± 6.2	-48.3 ± 22.8	526.0	51.9 ± 11.9	-20.7 ± 5.9	532.0
40	42.0 ± 3.7	41.8 ± 8.2	-45.7 ± 23.4	529.5	62.4 ± 13.0	-20.9 ± 6.8	535.5
50	47.1 ± 4.5	47.4 ± 11.8	-45.7 ± 17.8	533.0	69.8 ± 15.2	-19.9 ± 7.4	539.0
60	58.3 ± 4.6	55.8 ± 14.6	-42.8 ± 15.6	536.5	77.2 ± 19.3	-25.1 ± 6.6	542.5
80	76.8 ± 6.4	77.5 ± 16.6	-50.2 ± 22.8	546.5	106.5 ± 29.1	-24.2 ± 6.6	553.0
100	110.6 ± 8.5	106.6 ± 34.1	-44.2 ± 14.5	556.5	137.6 ± 43.4	-20.5 ± 8.2	561.3
150	149.1±11.9	139.3 ± 40.8	-44.1 ± 15.2	586.0	174.3 ± 57.5	-21.4 ± 7.4	597.5

218 DLS was used for an in-depth study of the PC and to determine variations in the hydrodynamic

219 diameter (HD) of the samples. Obtained results are summarized in **Table 1** and **Figure 4**, where it can

220 be seen how the HD of the AuNPs systematically increases after their exposure to cCCM, which is

221 associated with the direct adsorption of the proteins onto the surface of the NPs **(Fig. 4-A, B)**. This

222 increase strongly depends on the NP size and can be directly correlated with the thickness of the PC

223 (thickness = 1/2 ΔHD) **(Fig. 4-C, D)**. Thus, for small 3.5 nm AuNPs a protein layer of ~2.5 nm in

224 thickness is observed (ΔHD ~5 nm). As the size of the particles progressively increases the protein

225 coating becomes thicker, reaching a rather constant value of 8-10 nm (ΔHD from 16 to 20 nm) for

226 AuNPs from 12 to 80 nm. Finally, for particles larger than 80 nm, the thickness of the corona seems

227 to be even larger, obtaining an increase of 15-16 nm in thickness (ΔHD from 30 to 32 nm).

228 Considering the results obtained earlier and assuming that albumin (65 kDa, HD ~6-7 nm) and other

229 high molecular mass (>65 kDa) proteins[13] have been extensively found as the major constituents of

230 the PC, it is reasonable to identify three different regimes: (i) small size regime, where the particles

231   are smaller than mentioned proteins, and the thickness of the PC is thinner than that of a single layer

232   of proteins, (ii) medium size regime, where the size of the particles starts to be significantly larger

233   than of the proteins, and where the obtained thickness of the PC supports the overall formation of a

234   single layer of proteins and (iii) large size regime, where the size of the particles is much larger than

235   that of proteins, approaching a flat surface, and where the obtained PC thickness suggests the

236   formation of a multilayer of proteins. It is worth noting that despite the PC not being completely

237   developed in the small AuNP regime; it is robust and provides enough stability to prevent them from
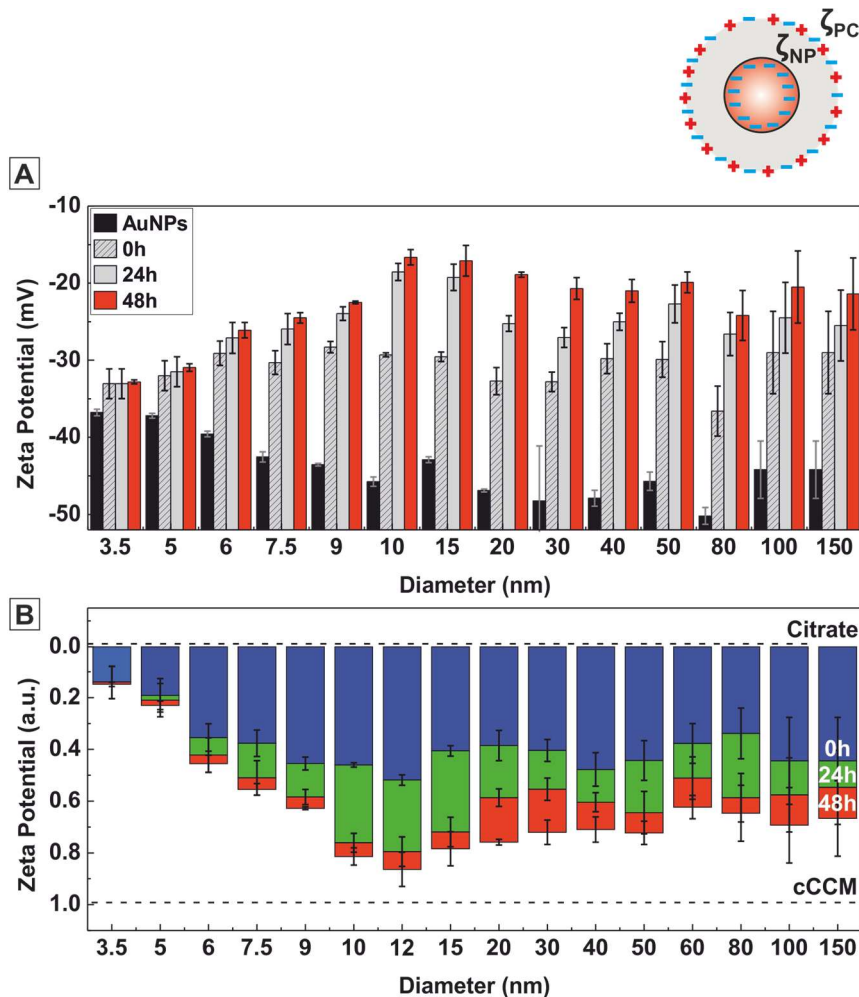
238   aggregation.

239

240   **Figure 4. Hydrodynamic diameter (HD) measured by dynamic light scattering of purified AuNPs of**

241   **different sizes after their exposure to cCCM for different times.** (A) HD obtained by DLS for particles

242   between 3.5 and 150 nm and (B) detailed for particles between 3.5 and 20 nm. (C, D) Respective increases in the

243   HD showing doubling of the corona thickness. Straight lines indicate different tendencies in the resultant protein

244   corona.

245   Similar evidence was obtained by zeta potential measurements used to assess the changes in particle

246   surface charge after exposure to cCCM. Thus, concomitant with the observed red-shift of the LSPR

247   position and the increase of the NP size measured by DLS, a drop in absolute surface charge of the

248   particles toward the average value of the medium proteins was systematically observed. It accounts

249   for the progressive screening of the negatively charged citrate-metal surface by the coating protein

250   layer, which provides a long-term colloidal stability to the AuNPs in biological media. Interestingly,

251   here again, zeta potential results depend on AuNP size (**Fig. 5A**), changing from -40 mV (citrate) to -

252   30 mV for the smallest particles, and to -(15-20) mV for larger particles after protein coating. These

253   results supports the previous idea that proteins are unable to form a dense layer on the surface of very

254 small AuNPs, while a proper protein corona is formed in the large ones, either by a single dense

255 protein layer or a multilayered coating. Since the surface charge itself is not high enough to prevent

256 NPs from electrostatic aggregation (an absolute value of 30 mV is usually considered a limit for

257 particle stability), these results are further evidence that the stability of the NPs is mediated by steric

258 repulsion provided by proteins (which stay in their native state[27]) rather than via the former
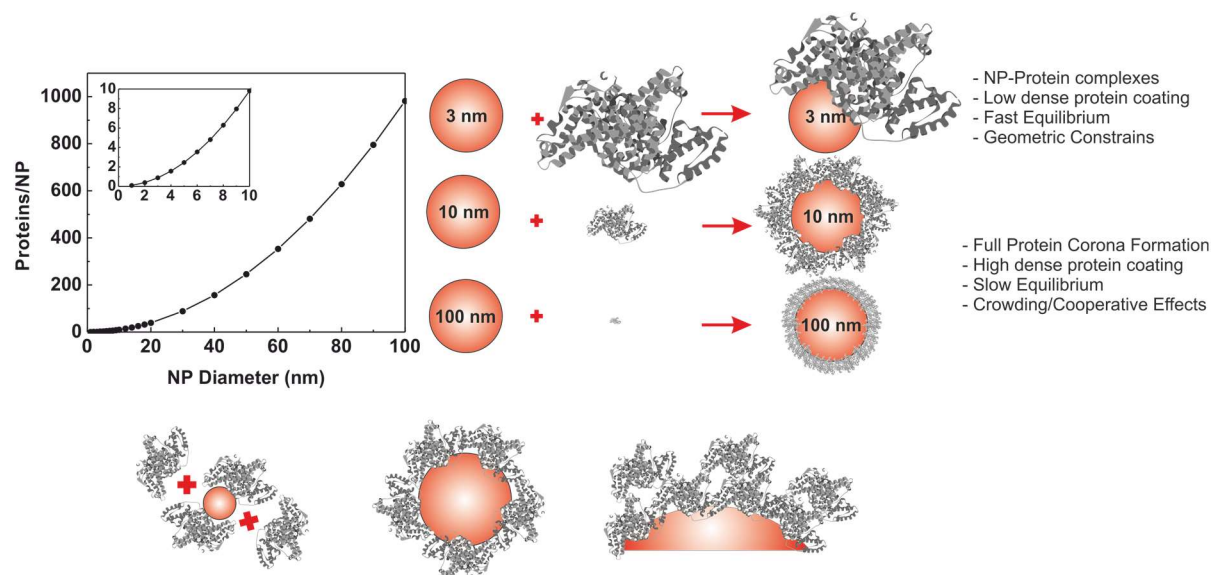
259 electrostatic repulsion provided by citrate.

260 As previously observed by UV-vis spectroscopy, time-dependent DLS and zeta potential results

261 confirm the kinetic evolution of a hard protein corona and its dependence on particle size **(Fig. 4** and

262 **Fig. 5)**, being faster (24 h) for smaller sizes than for larger ones (48 h). These results suggest that

263 particle size plays a critical role in both the kinetic and the thickness of the protein layer: the smaller

264 the particle the faster the kinetics evolution and the thinner (incomplete) the protein layer.

265

Figure 5. Zeta potential of purified AuNPs of different sizes after their exposure to cCCM for different
times. (A) Absolute values of zeta potential measurements and (B) relative values in which 0 represents the
surface charge of the citrate coated particles and 1 the charge of the proteins. The size-dependent protein corona
evolution is clearly observed; where small particles present the most negative charge after exposure as a
consequence of not forming a dense layer. For large particles, zeta potential is closer to that of the proteins
indicating the formation of a denser layer.

272   Based on the obtained results, there seems to be a size limit below which a complete PC cannot fully

273   develop. Presumably, this can be related to geometric constraints or other effects (crowding,

274   cooperative effects) that could be a subject of further studies. As described by Nygren and

275   Alaeddine,[57] and contrary to what might be expected, proteins do not distribute on surfaces randomly.

276   Instead, once the first proteins are attached they serve as nucleation centers for the deposition on new

277   ones, thereby stabilizing them, and this mechanism is repeated until the entire surface is filled. These

278   and other attempts to explain the irreversibility of this process seem to have in common that the initial

279   attachment of a protein to a surface is followed by a series of movements and/or rearrangements to

280   make the interaction more stable, ultimately resulting in an irreversible attachment. These processes

281   appear to be restricted when the particles become very small and their surface is limited to very few

282   proteins per NP (**Fig. 6**). On the other hand, the formation of a hard protein corona composed of more

283   than one layer of proteins is a plausible explanation for larger particles. In this case, when

284   approaching flat surfaces, proteins are subjected to larger conformational changes upon adsorption

285   leading to multiple protein adsorptions. Thus, the increase in the corona thickness of the larger

286   particles with respect to the smaller particles could be related to this effect along with the appearance

287   of defects on the first protein layer docking other proteins (**Fig. 6**). However, it remains unknown

288   whether particle size determines the nature of the PC only quantitatively (the number of proteins

289   attached) or also in a qualitatively way (the composition of proteins).[15]

290   In order to see whether and how obtained results can be extrapolated to other systems we studied the

291   PC formation in the presence of pure albumin. Considering the high abundance of albumin in serum

292

293   **Figure 6. Representative scheme of the formation process of a hard protein corona in citrate-stabilized**
294   **AuNPs of different sizes.** (i) NP-protein complexes (or incomplete coating), (ii) the formation of a single dense
295   protein corona layer and (iii) the formation of a multilayer corona. Graphic on the left details the number of
296   proteins that can attach on the surface of the NP as a single monolayer. Calculations has been performed based
297   on the size of BSA chosen as model protein (see SI).

298 (represents ~60% of the total mass serum proteins), its high affinity for many different surfaces, and

299 low specificity, albumin is known to be one of the main components of the protein corona when

300 AuNPs, and other NPs, are exposed to serum or blood plasma.[15, 25] Indeed, this high affinity of

301 albumin for gold surfaces has been widely proven, resulting in the spontaneous formation of a dense

302 and tightly bound albumin-rich coating in a process usually known as albuminization.[41, 49, 51, 58, 59]

303 With the aim to elucidate whether the albuminization of the particles showed similar size dependent

304 effects to those observed in the PC formation by serum proteins, analogous experiments were

305 performed by exposing the particles to BSA in phosphate buffer solution. The obtained results are

306 summarized in **Table 2**, confirming the formation of an irreversible BSA coating layer onto all the

307 citrate-stabilized AuNPs after 48 h of exposure. BSA adsorption did not induce colloidal aggregation

308 of the NPs, comparable to that given by FBS serum proteins in cCCM. This further indicates that the

309 BSA preserves their native state and do not undergo denaturalization. The obtained results are in

310 general agreement with those observed in the case of cCCM suggesting that BSA is unable to form a

311 proper corona for the very small particles while a single layer or multilayer is formed on larger ones.

312 Slight differences observed between FBS and BSA may account for the presence of other proteins in

313 combination with BSA. Briefly, the differences in the shift of the LSPR position (smaller in the case

314 of BSA than FBS) along with the variations of the HD observed by DLS (smaller in the case of BSA

315 than FBS) suggest that the presence of pure BSA may lead to the formation of a more structured, and

316 consequently thinner, layer.

317 **Table 2. Physicochemical Characterization of AuNPs before and after Exposure to BSA for 48 h and**
318 **Further Purified.**

Target Size (nm)	BSA		
	Diameter DLS (nm)	ζ-Potential (mV)	LSPR maximum (nm)
3.5	9.6 ± 1.6	-30.7 ± 7.3	513.5
5	10.6 ± 1.7	-29.5 ± 6.8	518.0
6	12.6 ± 2.5	-27.7 ± 4.5	520.0
7.5	14.9 ± 3.4	-23.5 ± 6.1	522.5
9	19.8 ± 4.4	-23.5 ± 4.7	522.5
10	22.2 ± 5.1	-18.5 ± 4.4	523.0
12	22.3 ± 5.2	-20.8 ± 5.2	522.5
15	29.6 ± 6.7	-21.9 ± 5.1	524.5
20	34.8 ± 7.8	-19.7 ± 6.8	527.5
30	44.4 ± 10.8	-21.8 ± 7.4	531.0
40	56.1 ± 11.0	-25.1 ± 6.6	534.0
50	60.9 ± 13.2	-22.2 ± 5.3	536.5
60	69.5 ± 19.3	-23.4 ± 5.9	540.5
80	98.3 ± 19.1	-25.2 ± 6.1	550.5
100	135.6 ± 35.4	-22.5 ± 7.7	560.5
150	159.1 ± 53.2	-24.6 ± 7.6	594.0

319

Conclusions

The optimization of exposure conditions (stability and purification) allowed us the study of the protein corona in citrate-stabilized AuNPs of different sizes. The proper combination of UV-vis spectroscopy, DLS, and zeta potential measurements has been proven as a potential tool to describe qualitatively the protein corona formation on the surface of AuNPs. These techniques need to be discussed together in order to avoid misleading interpretations. For example, the largest red-shift in the LSPR, measured by UV-vis is observed for the smallest particles, while DLS measurements show that these small particles form the thinnest corona. On the other hand, UV-vis spectroscopy and zeta potential do not predict the formation of a multilayer protein coating while DLS allows characterization of this process. Finally, all three techniques are effective in monitoring kinetic protein adsorption profiles. As a result we observed how both the kinetics of protein corona hardening and the characteristics of the protein corona are particle size-dependent, despite the question of debate remaining whether particle size determines the PC not only quantitatively but also in a qualitatively way.

The obtained results present relevant biological consequences as different NP–biological interactions take place at different time scales. Thus, tightly associated proteins may stay adherent to the particle when the particle is endocytosed from the extracellular fluid to an intracellular location, whereas proteins with a fast exchange rate are replaced by intracellular proteins during or after such a transfer. As a result, the same NP can give different biological responses depending on the portal of entry, history and preincubation in serum among others, thereby illustrating the importance of the study of size-dependences of the protein corona in a biological environment.

Experimental

Chemicals. Sodium citrate tribasic dihydrate (≥99%) and gold (III) chloride trihydrate HAuCl$_4$ · 3H$_2$O (99.9% purity) were purchased from Sigma-Aldrich. Fetal Bovine Serum, FBS (research grade, sterile filtered) and Dulbecco's Modified Eagle Medium, DMEM (with 1000 mg/mL glucose and sodium bicarbonate, whiteout L-glutamine, sodium pyruvate, and phenol red, liquid, sterile-filtered), were purchased from Sigma. All reagents were used as received without further purification and all glass material was sterilized and dehydrogenated in an oven prior to use. Milli-Q water was used in the preparation of all solutions.

Nanoparticle Synthesis. Aqueous solutions of citrate-stabilized AuNPs with different sizes (3.5-150 nm) were synthesized according to the previously developed seeded-growth method in our group. Detailed synthetic procedure and full characterization of the resultant solutions can be found in the respective articles.[47, 48] Briefly, AuNPs with increasing sizes were obtained from an initial AuNP solution after different sequential steps of growth; consisting of sample dilution plus further addition of gold precursor. This means that the number of particles in the solution decreases as the size

355 increases. Consequently, the concentration of smallest particles was ~10^{14}, which decreased down to

356 ~10^{10} for the largest 150 nm particles. All the particles were used within 20 days after synthesis. The

357 use of aged particles may result in increased experimental variability, since after a large period of time

358 the stability of the particles may be compromised by the degradation of the surfactant.

359 **Exposure to Cell Culture Media.** Complete cell culture medium (cCCM) consisted of DMEM

360 supplemented with 10% of FBS. AuNPs and cCMM were mixed (1:10 by volume) and placed in an

361 incubator at 37^0C for different incubation times. As a result, the final concentration of AuNPs was

362 that of the synthesis divided by the dilution factor: ~10^{13} NP/mL for the smallest particles and ~10^9

363 for the largest particles (approximately 0.05 mM of Au). At these working concentrations, AuNPs

364 were stable throughout the experiments and the number of proteins in larger excess with respect to the

365 available particle surface area. After incubation, the samples were centrifuged between 2000 and

366 35000 g for 10-20 min. (the larger the size, the lower the speed) to remove the excess of unbound or

367 loosely bound proteins on the NP surfaces followed by resuspension in the particle original medium

368 (sodium citrate 2.2 mM). Any possible aggregated fraction resulting from the centrifugation process

369 was removed by filtering the samples with a 200 nm-pore-size cellulose acetate membrane. In the

370 case in which the AuNPs solution needed to be concentrated with respect to the synthesis

371 concentration, such as for stability tests, a regenerated cellulose centrifugal filter (Millipore 10KDa)

372 was used.

373 **Physicochemical Characterization of the NPs and NP-Protein Corona**. AuNPs and the time

374 evolution of their coating by proteins were characterized before and after exposure to cCCM using

375 different techniques. The proper combination of these techniques has been used in other similar

376 studies by our group[27] and proven to be reliable when performed with adequate controls. *TEM:*

377 Diameter of the synthetized particles were obtained from analysis of TEM images acquired with a

378 JEOL 10101 electron microscope operating at an accelerating voltage of 80 kV. Samples were

379 prepared by drop-casting 10 microliter of the sample on a carbon-coated copper TEM grid and left to

380 dry at room temperature. At least 500 particles from different regions of the grid were counted. In

381 order to avoid aggregation of the particles during TEM grid preparation they were previously

382 conjugated with 11-mercaptoundecanoic acid. *UV-Visible Spectroscopy:* UV-Visible spectra were

383 acquired with a Shimadzu UV-2400 spectrophotometer. 1 mL of sample was placed in a plastic

384 cuvette, and spectral analysis was performed in the 300 to 800 nm range at room temperature. AuNPs

385 exhibit a characteristic absorbance peak in this region, the so-called localized surface plasmon

386 resonance (LSPR) band. The LSPR position is sensitive to the surrounding of the NPs at the

387 molecular level, and therefore the changes in the close environment of the NPs (such as the protein

388 adsorption) can be investigated using this technique. Water was taken as the reference for all samples.

389 *DLS and zeta potentia measurements:* The hydrodynamic size and surface charge of the AuNPs

390 before and after incubation in cCCM were determined by Dynamic Light Scattering (number mean)

391   and Laser Doppler Anemometry respectively, using a Zetasizer Nano ZS instrument equipped with a

392   light source wavelength of 532 nm and a fixed scattering angle of 173^0. Aliquots (0.8 mL) of the

393   colloidal NP solutions were placed into specific plastic cuvette and the software was arranged with the

394   parameters of refractive index and adsorption coefficient of gold, and solvent viscosity of water at 25

395   ^{0}C. Each value was the average of at least 3 independent measurements.

Supporting Information

405   Full characterization of the cell culture media by UV-vis spectroscopy, dynamic light scattering and

406   zeta potential, verification of the excess of proteins compared to the surface area of the nanoparticles

407   and detailed purification steps of the particles.

References

(1)   Sperling, R. A., Rivera Gil, P., Zhang, F., Zanella, M., and Parak, W. J. (2008) Biological applications of gold nanoparticles. *Chem. Soc. Rev 37*, 1896-1908.

(2)   Ghosh, P., Han, G., De, M., Kim, C. K., and Rotello, V. M. (2008) Gold nanoparticles in delivery applications. *Adv. Drug. Deliv. Rev. 60*, 1307-15.

(3)   Krug, H. F. (2014) Nanosafety Research-Are We on the Right Track? *Angew. Chem., Int. Ed. 53*, 12304-12319.

(4)   Nel, A. E., Madler, L., Velegol, D., Xia, T., Hoek, E. M., Somasundaran, P., Klaessig, F., Castranova, V., and Thompson, M. (2009) Understanding biophysicochemical interactions at the nano-bio interface. *Nat. Mater. 8*, 543-57.

(5)   Moyano, D. F., and Rotello, V. M. (2011) Nano Meets Biology: Structure and Function at the Nanoparticle Interface. *Langmuir 27*, 10376-10385.

(6)   Saptarshi, S. R., Duschl, A., and Lopata, A. L. Interaction of nanoparticles with proteins: relation to bio-reactivity of the nanoparticle. *J. Nanobiotechnol. 11*, 26.

(7)   Cedervall, T., Lynch, I., Lindman, S., Berggard, T., Thulin, E., Nilsson, H., Dawson, K. A., and Linse, S. (2007) Understanding the nanoparticle-protein corona using methods to quantify exchange rates and affinities of proteins for nanoparticles. *Proc. Natl. Acad. Sci.U. S. A 104*, 2050-2055.

(8)   Walkey, C. D., Olsen, J. B., Song, F., Liu, R., Guo, H., Olsen, D. W. H., Cohen, Y., Emili, A., and Chan, W. C. W. (2014) Protein Corona Fingerprinting Predicts the Cellular Interaction of Gold and Silver Nanoparticles. *ACS Nano 8*, 2439-2455.

(9)   Hamad-Schifferli, K. (2015) Exploiting the novel properties of protein coronas: emerging applications in nanomedicine. *Nanomedicine 10*, 1663-1674.

(10)   Casals, E., and Puntes, V. F. (2012) Inorganic nanoparticle biomolecular corona: formation, evolution and biological impact. *Nanomedicine (Lond) 7*, 1917-30.

(11) Mahmoudi, M., Lynch, I., Ejtehadi, M. R., Monopoli, M. P., Bombelli, F. B., and Laurent, S. (2011) Protein−Nanoparticle Interactions: Opportunities and Challenges. *Chem. Rev. 111*, 5610-5637.

(12) Wilson, C. J., Clegg, R. E., Leavesley, D. I., and Pearcy, M. J. (2005) Mediation of biomaterial-cell interactions by adsorbed proteins: a review. *Tissue Eng. 11*, 1-18.

(13) Monopoli, M. P., Aberg, C., Salvati, A., and Dawson, K. A. (2012) Biomolecular coronas provide the biological identity of nanosized materials. *Nat. Nanotechnol. 7*, 779-786.

(14) Walczyk, D., Bombelli, F. B., Monopoli, M. P., Lynch, I., and Dawson, K. A. (2010) What the Cell "Sees" in Bionanoscience. *J. Am. Chem. Soc. 132*, 5761-5768.

(15) Tenzer, S., Docter, D., Kuharev, J., Musyanovych, A., Fetz, V., Hecht, R., Schlenk, F., Fischer, D., Kiouptsi, K., Reinhardt, C., Landfester, K., Schild, H., Maskos, M., Knauer, S. K., and Stauber, R. H. (2013) Rapid formation of plasma protein corona critically affects nanoparticle pathophysiology. *Nat. Nanotechnol. 8*, 772-U1000.

(16) Saha, K., Rahimi, M., Yazdani, M., Kim, S. T., Moyano, D. F., Hou, S., Das, R., Mout, R., Rezaee, F., Mahmoudi, M., and Rotello, V. M. (2016) Regulation of Macrophage Recognition through the Interplay of Nanoparticle Surface Functionality and Protein Corona. *ACS Nano 10*, 4421-4430.

(17) Salvati, A., Pitek, A. S., Monopoli, M. P., Prapainop, K., Bombelli, F. B., Hristov, D. R., Kelly, P. M., Aberg, C., Mahon, E., and Dawson, K. A. (2013) Transferrin-functionalized nanoparticles lose their targeting capabilities when a biomolecule corona adsorbs on the surface. *Nat. Nanotechnol. 8*, 137-143.

(18) Jiang, Y., Wang, M., Hardie, J., Tonga, G. Y., Ray, M., Xu, Q. B., and Rotello, V. M. (2016) Chemically Engineered Nanoparticle-Protein Interface for Real-Time Cellular Oxidative Stress Monitoring. *Small 12*, 3775-3779.

(19) Corbo, C., Molinaro, R., Parodi, A., Furman, N. E. T., Salvatore, F., and Tasciotti, E. (2016) The impact of nanoparticle protein corona on cytotoxicity, immunotoxicity and target drug delivery. *Nanomedicine 11*, 81-100.

(20) Miclaus, T., Beer, C., Chevallier, J., Scavenius, C., Bochenkov, V. E., Enghild, J. J., and Sutherland, D. S. (2016) Dynamic protein coronas revealed as a modulator of silver nanoparticle sulphidation in vitro. *Nat. Commun. 7,* 11770.

(21) Saha, K., Moyano, D. F., and Rotello, V. M. (2014) Protein coronas suppress the hemolytic activity of hydrophilic and hydrophobic nanoparticles. *Mater. Horiz. 1*, 102-105.

(22) Maiorano, G., Sabella, S., Sorce, B., Brunetti, V., Malvindi, M. A., Cingolani, R., and Pompa, P. P. (2010) Effects of Cell Culture Media on the Dynamic Formation of Protein−Nanoparticle Complexes and Influence on the Cellular Response. *ACS Nano 4*, 7481-7491.

(23) Monopoli, M. P., Walczyk, D., Campbell, A., Elia, G., Lynch, I., Baldelli Bombelli, F., and Dawson, K. A. (2011) Physical−Chemical Aspects of Protein Corona: Relevance to in Vitro and in Vivo Biological Impacts of Nanoparticles. *J. Am. Chem. Soc. 133*, 2525-2534.

(24) Casals, E., Pfaller, T., Duschl, A., Oostingh, G. J., and Puntes, V. F. (2011) Hardening of the Nanoparticle-Protein Corona in Metal (Au, Ag) and Oxide (Fe3O4, CoO, and CeO2) Nanoparticles. *Small 7*, 3479-3486.

(25) Tenzer, S., Docter, D., Rosfa, S., Wlodarski, A., Kuharev, J., Rekik, A., Knauer, S. K., Bantz, C., Nawroth, T., Bier, C., Sirirattanapan, J., Mann, W., Treuel, L., Zellner, R., Maskos, M., Schild, H., and Stauber, R. H. (2011) Nanoparticle Size Is a Critical Physicochemical Determinant of the Human Blood Plasma Corona: A Comprehensive Quantitative Proteomic Analysis. *ACS Nano 5*, 7155-7167.

(26) Walkey, C. D., Olsen, J. B., Guo, H., Emili, A., and Chan, W. C. W. (2012) Nanoparticle Size and Surface Chemistry Determine Serum Protein Adsorption and Macrophage Uptake. *J. Am. Chem. Soc. 134*, 2139-2147.

(27) Casals, E., Pfaller, T., Duschl, A., Oostingh, G. J., and Puntes, V. (2010) Time Evolution of the Nanoparticle Protein Corona. *ACS Nano 4*, 3623-3632.

(28) Gessner, A., Waicz, R., Lieske, A., Paulke, B. R., Mader, K., and Muller, R. H. (2000) Nanoparticles with decreasing surface hydrophobicities: influence on plasma protein adsorption. *Int. J. Pharm. 196*, 245-249.

(29) Slack, S. M., and Horbett, T. A. (1995) The Vroman Effect, in *Proteins at Interfaces II* pp 112-128, American Chemical Society.

(30) Hill, H. D., Millstone, J. E., Banholzer, M. J., and Mirkin, C. A. (2009) The Role Radius of Curvature Plays in Thiolated Oligonucleotide Loading on Gold Nanoparticles. *ACS Nano 3*, 418-424.

(31) Walkey, C. D., and Chan, W. C. W. (2012) Understanding and controlling the interaction of nanomaterials with proteins in a physiological environment. *Chem. Soc. Rev 41*, 2780-2799.

486   (32) Cedervall, T., Lynch, I., Foy, M., Berggad, T., Donnelly, S. C., Cagney, G., Linse, S., and Dawson, K. A.
487   (2007) Detailed identification of plasma proteins adsorbed on copolymer nanoparticles. *Angew. Chem., Int.*
488   *Ed. 46*, 5754-5756.

489   (33) Dobrovolskaia, M. A., Patri, A. K., Zheng, J., Clogston, J. D., Ayub, N., Aggarwal, P., Neun, B. W., Hall,
490   J. B., and McNeil, S. E. (2009) Interaction of colloidal gold nanoparticles with human blood: effects on
491   particle size and analysis of plasma protein binding profiles. *Nanomedicine 5*, 106-117.

492   (34) Mahmoudi, M., Lohse, S. E., Murphy, C. J., Fathizadeh, A., Montazeri, A., and Suslick, K. S. (2014)
493   Variation of Protein Corona Composition of Gold Nanoparticles Following Plasmonic Heating. *Nano Lett.*
494   *14*, 6-12.

495   (35) Deng, Z. J., Liang, M. T., Toth, I., Monteiro, M., and Minchin, R. F. (2013) Plasma protein binding of
496   positively and negatively charged polymer-coated gold nanoparticles elicits different biological responses.
497   *Nanotoxicol. 7*, 314-322.

498   (36) Lundqvist, M., Stigler, J., Elia, G., Lynch, I., Cedervall, T., and Dawson, K. A. (2008) Nanoparticle size
499   and surface properties determine the protein corona with possible implications for biological impacts.
500   *Proc. Natl. Acad. Sci.U. S. A 105*, 14265-14270.

501   (37) Ehrenberg, M. S., Friedman, A. E., Finkelstein, J. N., Oberdorster, G., and McGrath, J. L. (2009) The
502   influence of protein adsorption on nanoparticle association with cultured endothelial cells. *Biomaterials 30*,
503   603-610.

504   (38) Gessner, A., Lieske, A., Paulke, B. R., and Muller, R. H. (2003) Functional groups on polystyrene model
505   nanoparticles: Influence on protein adsorption. *J. Biomed. Mater. Res. A 65*, 319-326.

506   (39) Sund, J., Alenius, H., Vippola, M., Savolainen, K., and Puustinen, A. (2011) Proteomic Characterization of
507   Engineered Nanomaterial-Protein Interactions in Relation to Surface Reactivity. *ACS Nano 5*, 4300-4309.

508   (40) Deng, Z. J., Mortimer, G., Schiller, T., Musumeci, A., Martin, D., and Minchin, R. F. (2009) Differential
509   plasma protein binding to metal oxide nanoparticles. *Nanotechnol. 20*.

510   (41) Roecker, C., Poetzl, M., Zhang, F., Parak, W. J., and Nienhaus, G. U. (2009) A quantitative fluorescence
511   study of protein monolayer formation on colloidal nanoparticles. *Nat. Nanotechnol. 4*, 577-580.

512   (42) Treuel, L., Brandholt, S., Maffre, P., Wiegele, S., Shang, L., and Nienhaus, G. U. Impact of Protein
513   Modification on the Protein Corona on Nanoparticles and Nanoparticle-Cell Interactions. *ACS Nano 8*,
514   503-513.

515   (43) Bastus, N. G., Sanchez-Tillo, E., Pujals, S., Farrera, C., Lopez, C., Giralt, E., Celada, A., Lloberas, J., and
516   Puntes, V. (2009) Homogeneous conjugation of peptides onto gold nanoparticles enhances macrophage
517   response. *ACS Nano 3*, 1335-44.

518   (44) Banerjee, T., Mitra, S., Singh, A. K., Sharma, R. K., and Maitra, A. (2002) Preparation, characterization
519   and biodistribution of ultrafine chitosan nanoparticles. *Int. J. Pharm. 243*, 93-105.

520   (45) Choi, H. S., Liu, W., Misra, P., Tanaka, E., Zimmer, J. P., Ipe, B. I., Bawendi, M. G., and Frangioni, J. V.
521   (2007) Renal clearance of quantum dots. *Nat. Biotechnol. 25*, 1165-1170.

522   (46) Gebauer, J. S., Malissek, M., Simon, S., Knauer, S. K., Maskos, M., Stauber, R. H., Peukert, W., and
523   Treuel, L. (2012) Impact of the Nanoparticle–Protein Corona on Colloidal Stability and Protein Structure.
524   *Langmuir 28*, 9673-9679.

525   (47) Piella, J., Bastús, N. G., and Puntes, V. (2016) Size-Controlled Synthesis of Sub-10-nanometer Citrate-
526   Stabilized Gold Nanoparticles and Related Optical Properties. *Chem. Mater. 28*, 1066-1075.

527   (48) Bastús, N. G., Comenge, J., and Puntes, V. F. (2011) Kinetically Controlled Seeded Growth Synthesis of
528   Citrate-Stabilized Gold Nanoparticles of up to 200 nm: Size Focusing versus Ostwald Ripening. *Langmuir*
529   *27*, 11098-11105.

530   (49) Goy-López, S., Juárez, J., Alatorre-Meda, M., Casals, E., Puntes, V. F., Taboada, P., and Mosquera, V.
531   (2012) Physicochemical Characteristics of Protein–NP Bioconjugates: The Role of Particle Curvature and
532   Solution Conditions on Human Serum Albumin Conformation and Fibrillogenesis Inhibition. *Langmuir*
533   *28*, 9113-9126.

534   (50) Comenge, J. (2015) The Role of PEG Conformation in Mixed Layers: From Protein Corona Substrate to
535   Steric Stabilization Avoiding Protein Adsorption.

536   (51) Dominguez-Medina, S., McDonough, S., Swanglap, P., Landes, C. F., and Link, S. (2012) In Situ
537   Measurement of Bovine Serum Albumin Interaction with Gold Nanospheres. *Langmuir 28*, 9131-9139.

538   (52) Casals, E., Pfaller, T., Duschl, A., Oostingh, G. J., and Puntes, V. (2010) Time evolution of the
539   nanoparticle protein corona. *ACS Nano 4*, 3623-32.

540   (53) Saha, K., Agasti, S. S., Kim, C., Li, X., and Rotello, V. M. (2012) Gold Nanoparticles in Chemical and
541   Biological Sensing. *Chem. Rev. 112*, 2739-2779.

542   (54) Lévy, R., Thanh, N. T. K., Doty, R. C., Hussain, I., Nichols, R. J., Schiffrin, D. J., Brust, M., and Fernig,
543   D. G. (2004) Rational and Combinatorial Design of Peptide Capping Ligands for Gold Nanoparticles. *J.*
544   *Am. Chem. Soc. 126*, 10076-10084.

545   (55) Zook, J. M., MacCuspie, R. I., Locascio, L. E., Halter, M. D., and Elliott, J. T. (2011) Stable nanoparticle
546   aggregates/agglomerates of different sizes and the effect of their size on hemolytic cytotoxicity.
547   *Nanotoxicol. 5*, 517-530.

548   (56) Bastús, N. G., Piella, J., and Puntes, V. (2015) Quantifying the Sensitivity of Multipolar (Dipolar,
549   Quadrupolar, and Octapolar) Surface Plasmon Resonances in Silver Nanoparticles: The Effect of Size,
550   Composition, and Surface Coating. *Langmuir*.

551   (57) Alaeddine, S., and Nygren, H. (1995) Logarithmic Growth of Protein Films, in *Proteins at Interfaces II* pp
552   41-51, American Chemical Society.

553   (58) Tsai, D.-H., DelRio, F. W., Keene, A. M., Tyner, K. M., MacCuspie, R. I., Cho, T. J., Zachariah, M. R.,
554   and Hackley, V. A. (2011) Adsorption and Conformation of Serum Albumin Protein on Gold
555   Nanoparticles Investigated Using Dimensional Measurements and in Situ Spectroscopic Methods.
556   *Langmuir 27*, 2464-2477.

557   (59) Brewer, S. H., Glomm, W. R., Johnson, M. C., Knag, M. K., and Franzen, S. (2005) Probing BSA Binding
558   to Citrate-Coated Gold Nanoparticles and Surfaces. *Langmuir 21*, 9303-9307.

Supporting information for:

Size-dependent Protein-Nanoparticle Interactions in Citrate-Stabilized Gold Nanoparticles: The Emergence of the Protein Corona.

Jordi Piella, Neus G. Bastús and Víctor Puntes

Table of Contents

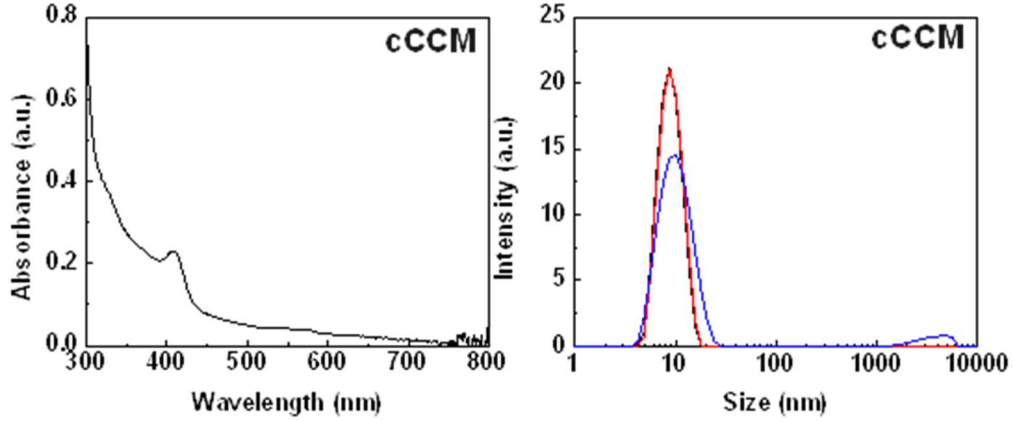# 1. Characterization of complete cell culture media (cCCM)

Figure S1. Characterization of complete cell culture media (cCCM): DMEM supplemented with 10% of FBS. UV-vis spectrum (left) shows a strong absorbance in the region below 500 nm, while almost no absorbance is observed above this value, where the Localized Surface Plasmon Resonance peak characteristic of the AuNPs is usually located. Dynamic light scattering plot (DLS) (right) of the cCCM displaying an intense peak in the region between 5 and 15 nm attributed to the proteins. This peak may overlap with the AuNPs peak if they have not been previously purified. Finally, the zeta potential of the cCCM results in -11.2 ± 0.9 mV which is characteristic of the slightly negative charge of most of the proteins.

2. Excess of proteins in cCCM compared to the total surface area of AuNPs

For a specific colloidal solution of AuNPs, the average NP diameter ($\bar{D}$), average NP surface area ($\bar{S}$) and average NP mass ($\bar{M}$) can be calculated from the size distribution obtained by TEM analysis:

$$\bar{D}\left(\frac{cm^2}{NP}\right) = \frac{\sum D_n}{n} \tag{1}$$

$$\bar{S}\left(\frac{cm^2}{NP}\right) = \frac{\pi}{4}\frac{\sum D_n{}^2}{n} \tag{2}$$

$$\bar{M}\left(\frac{mols}{NP}\right) = \bar{V}_{NP}\delta M_W = \frac{4}{3}\frac{\sum\left(\frac{D_n}{2}\right)^3}{n}\delta M_W \tag{3}$$

where n and D_n are the number and diameter of the particles that has been counted by TEM (at least 500 NPs are needed for a representative population), δ is the density of gold, 19.3 g/mL,

and M_w the molecular weight, MW 197. Notice that a common error is to calculate $\bar{S}$ and $\bar{M}$ from $\bar{D}$ (the polydispersity degree of the particles is erroneously omitted in this case). Finally, the concentration of gold (C_{Au}), obtained either from the concentration of precursor used in the synthesis of the particles and the yield of the reaction or by ICP-MS, can be translated to the number of NPs and the surface area in solution as follow:

$$number\ of\ NPs\ \left(\frac{NP}{L}\right) = concentration\ of\ Au\ (M) \cdot \frac{1}{\bar{M}}\left(\frac{mol}{NP}\right)^{-1} \qquad (4)$$

$$surface\ area\ \left(\frac{cm^2}{L}\right) = number\ of\ NP\left(\frac{NP}{L}\right) \cdot \bar{S}\left(\frac{cm^2}{NP}\right) \qquad (5)$$

The total surface area in a standard synthesis procedure range from 2 to 30 cm^2/mL, which corresponds to ~10^9 NPs/mL for the larger particles (150 nm) and to ~10^{13} for the smallest ones (3.5 nm).

On the other hand, the total number of proteins in cCCM is at least three orders of magnitude larger than that of the particles in solution. The total surface area they can cover upon adsorption on a surface is the result of multiplying their cross section (CS) for their concentration (C):

$$area_{proteins}\ \left(\frac{cm^2}{L}\right) = \Sigma\left(C_{protein} \cdot CS_{protein}\right) \qquad (6)$$

For example, the triangular CS of the BSA in the folded conformation has been previously estimated to be 32 nm^2 = 32·10^{-14} cm^2 while their concentration in the cCMM is around 6·10^{16} (0.1 mM). This represents enough BSA in the cCCM to cover a total area of 19300 (cm^2/mL); at least more than 5 10^2 times higher than that needed to fully surround the AuNPs surface in solution. Thus, it is reasonable to consider the number of proteins in the cCCM largely in excess with respect to the AuNPs, even if more than one layer of proteins is adsorbed on the surface of the particles, and the fraction depleted from the medium upon adsorption insignificant.

3. Number of washing steps for a proper DLS characterization

cCCM free of NPs gives a background peak in the range of 5-15 nm by DLS (see section 1), which is comparable to the hydrodynamic size of the small AuNPs used in the experiments here presented. Consequently, interferences from the unbounded proteins in solution when measuring the hydrodynamic size of the AuNPs by DLS is something that should not be ruled out if the particles has not been previously washed and dispersed in a solution free of proteins.

The interferences that free proteins in solution may induce to the DLS measurements[1] can be estimated from their respective abilities to scatter light assuming Rayleigh scattering properties, in which scattering intensity of a specific molecule is proportional to its number in solution (N) and its size raised to the six power (D^6):

$$I \propto \varepsilon \, N \, D^6 \tag{7}$$

where ε is the refractive index for each molecule. The relative contributions of the unbounded proteins with respect to the AuNPs can be then quantified by defining a dimensionless parameter (γ) as follow:

$$\gamma = \frac{I_{NP}}{I_p} = \frac{\varepsilon_{NP} N_{NP} D_{NP}{}^6}{\sum \varepsilon_P N_P D_P{}^6} = \frac{0.47 N_{NP} D_{NP}{}^6}{\sum \varepsilon_P N_P D_P{}^6} \tag{8}$$

where the refractive index for AuNP is $\varepsilon_{NP} = 0.47$, while the ε_P is ~ 1.5 for proteins. Previous studies with BSA have demonstrated that γ should be at least > 0.1 to avoid the contributions of free proteins in the DLS measurements.[1]

In this regard, rough calculations based on the approximate BSA concentration in cCCM ($6 \cdot 10^{16}$ protein/mL, HD 7 nm and $\varepsilon_P = 1.447$), demonstrated that $\gamma \ll 0.1$ for AuNPs of 3.6 nm in the range of concentration here working (10^{13} NP/mL) and at least 2 cycles of washing were needed to avoid the contribution of unbound proteins (note that each washing step consist on replacing 980 uL of supernatant from a 1000 uL of solution decreasing the concentration of proteins in

solution by a factor of 50x). Indeed, based on the previous approximation the concentration of these particles should be in the range of $1 \cdot 10^{18}$ to be properly measured in cCCM without requiring any washing step. On the other hand, γ already approach to that of 0.1 for AuNP of 60 nm at any concentration larger than $4 \cdot 10^{10}$, which is in the range of working concentration in our experiments. In agreement with that, DLS plot showed monomodal curves even in the absence of any washing steps for large AuNPs (Figure S2-S3).
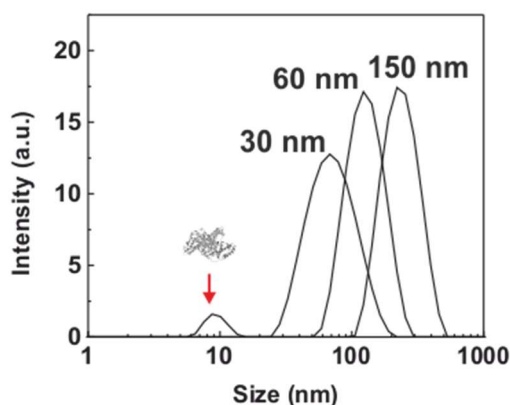

Figure S2. DLS plot of AuNPs measured in cCCM without purification of the particles. Particles of 60 nm and 150 nm show a monomodal curve, while particle of 30 nm, and below, present a bimodal curve due to interferences from unbound proteins in the medium.
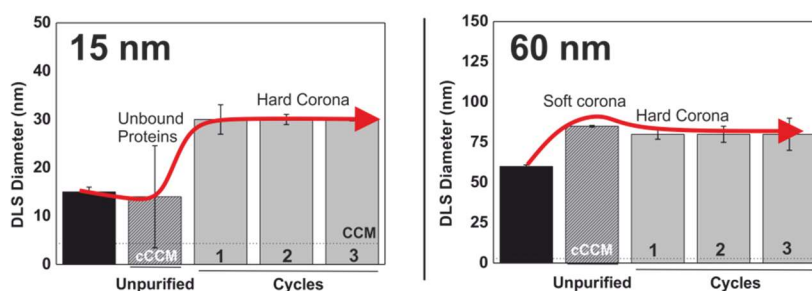

Figure S3. Hydrodynamic diameter measured by DLS. For 15 nm particles the measured diameter decreases after incubation in cCCM as a result of contributions from unbound proteins. For 60 nm particles unbound proteins in cCCM does not significantly contribute to the measured values.

4. Maximum number of proteins per NP considering a monolayer coating

The theoretical available number of binding sites (NBS) for a monolayer coverage of proteins (considering BSA as a model protein) on a NP with a diameter (D) is estimated by dividing the surface area of the NP (πD^2) by the triangular cross section of the folded BSA (32 nm^2):[2]

$$\frac{BSA}{NP} = \frac{CS_{BSA}}{\pi D^2} = \frac{32}{\pi D^2} \quad NBS = \frac{\pi D^2}{CS_{BSA}} = \frac{\pi D^2}{32} \tag{9}$$

References

(1)   Tsai, D.-H., DelRio, F. W., Keene, A. M., Tyner, K. M., MacCuspie, R. I., Cho, T. J., Zachariah, M. R., and Hackley, V. A. (2011) Adsorption and Conformation of Serum Albumin Protein on Gold Nanoparticles Investigated Using Dimensional Measurements and in Situ Spectroscopic Methods. *Langmuir 27*, 2464-2477.

(2)   Dominguez-Medina, S., McDonough, S., Swanglap, P., Landes, C. F., and Link, S. (2012) In Situ Measurement of Bovine Serum Albumin Interaction with Gold Nanospheres. *Langmuir 28*, 9131-9139.